



# HIGH-RESOLUTION FLY-OVER BEAMFORMING USING A PRACTICAL ARRAY

Yutaka Ishii<sup>1</sup>, Jørgen Hald<sup>2</sup>, Tatsuya Ishii<sup>3</sup>, Hideshi Oinuma<sup>3</sup>, Kenichiro Nagai<sup>3</sup>, Yuzuru Yokokawa<sup>3</sup> and Kazuomi Yamamoto

<sup>1</sup>Brüel & Kjaer Japan

Chiyoda-ku, 101-0048, Tokyo, Japan

<sup>2</sup>Brüel & Kjaer SVM A/S, Denmark

<sup>3</sup>Japan Aerospace Exploration Agency (JAXA), Japan

## ABSTRACT

In a previous paper presented at the AIAA 1012 Aeroacoustics Conference, the authors described a commercially available fly-over beamforming system based on a small practical 108-element array with 12 metre diameter designed for quick deployment on a concrete runway. However, the resolution at frequencies below 700 Hz was not sufficient to provide useful noise source identification and quantification. The present paper describes an extended 135-element array with 29 metre diameter, designed for frequencies down to 300 Hz, while still supporting quick deployment on a runway, and it analyzes the results from a series of measurements taken in November 2011 at Taiki Aerospace Research Field, Taiki, Hokkaido, Japan. As in the previous paper, the aircraft under test was a business jet type MU300 from Mitsubishi Heavy Industries. For comparison with engine sound power estimates from fly-over measurements, a set of array measurements was performed on the right engine with the aircraft fixed on the ground. Sound power spectra show good agreement between fly-over and ground-based measurements with comparable engine load conditions.

## 1 INTRODUCTION

In an earlier paper presented at the AIAA 2012 conference, [1], the authors described a commercially available fly-over beamforming system based on a small practical array designed for quick deployment on a concrete runway. The array consisted of 9 identical 6 metre long line arrays with integrated cabling and with 12 microphones on each line. The system was used for a series of fly-over measurements on a business jet type MU300 from Mitsubishi Heavy Industries in 2010, and the results from a couple of these measurements were presented in the paper. However, at frequencies lower than approximately 700 Hz the array diameter was too small to achieve useful noise source identification and quantification.

The authors therefore designed an extended array with 29 metre diameter and 135 microphones to achieve good resolution down to 300 Hz while still supporting quick deployment on a runway. The extended array was used in a series of fly-over measurements on

an MU300 business jet in November 2011 at Taiki Aerospace Research Field, Taiki, Hokkaido, Japan. For comparison, an additional set of array measurements was performed with the aircraft standing on the ground and with the engine on the right-hand side running under load conditions comparable to those during flight. The present paper introduces the two array systems used for fly-over measurements and for ground based measurements, and it presents some typical results. Particular focus is placed on the comparison of the sound power results from the fly-over and from the ground-based measurements.

## 2 FLY-OVER MEASUREMENTS

### 2.1 Method and System overview

Both the applied system design principles and the beamforming methodology are exactly the same as described in reference [1], except that each one of the 9 radial linear sub-arrays was extended by 3 microphones to comprise 15 microphones with exponentially increasing distances to the centre. As a result the array diameter was extended from 12 metre to 29 metre. Figure 1 illustrates the array geometry, while Fig. 2 contains a picture of the central part of the array on the runway with an added picture of the centre plate that holds the line arrays at the centre. The centre plate, the line arrays and the arcs between them define quite precisely the xy-positions of the microphones in a horizontal plane. The vertical positions were calculated from the xy-coordinates and the measured slopes of planar sections of the runway.

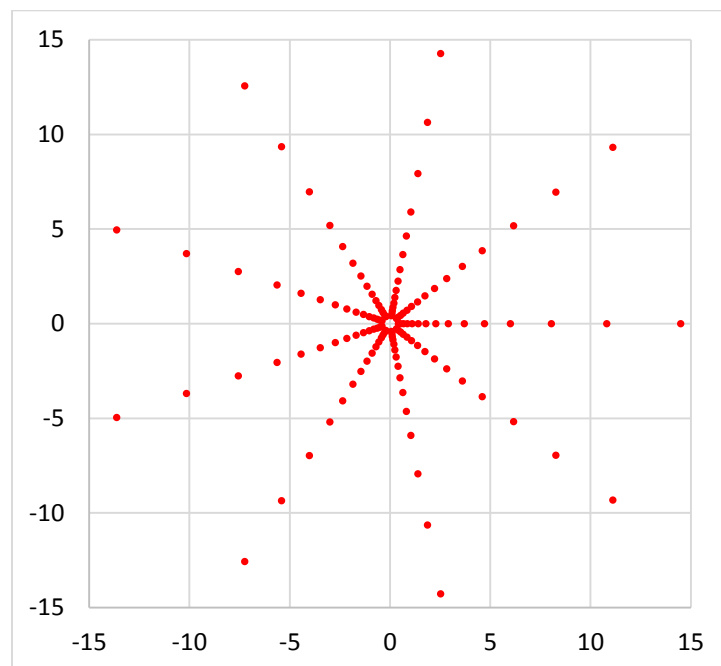


*Fig. 1. The applied array geometry consisting of 9 identical line arrays with 15 microphones on each line. The microphones have exponentially increasing distances to the centre.*

The applied method follows the same overall measurement and processing scheme as the hybrid time-frequency approach described in reference [2]. Aircraft position during a fly-over is measured with an onboard GPS system together with speed, roll, yaw and pitch. Synchronization with array data is achieved through recording of an IRIG-B time-stamp signal

together with the array data and also with the GPS data on the aircraft. The beamforming calculation is performed with a standard tracking time-domain Delay And Sum algorithm [3]. For each focus point in the moving system, FFT and averaging is then performed in short time intervals to obtain spectral noise source maps representing the aircraft positions at the middle of the averaging intervals. Diagonal Removal is implemented as described in reference [3], providing the capability of suppressing the contributions to the averaged spectra from the wind noise in the individual microphones. With sufficiently short averaging intervals, the response to a point source, i.e. the Point Spread Function, will remain almost constant during the corresponding sweep of each focus point. This means that a deconvolution calculation can be performed for each FFT frequency line and for each averaging interval in order to enhance resolution, suppress sidelobes and scale the maps. For this purpose, the FFT-NNLS algorithm described for example in reference [4] was used.



*Fig. 2. Central array section on the runway with an added picture of the centre plate. Each line array with integrated cabling contains here 12 microphones. To extend the array diameter, 3 extra microphones were added to each line. The 3 microphones on one extension were attached to a wire that controlled the microphone spacings and the distance to the central array section.*

Compensation for wind was performed using a simple model assuming a constant wind direction and speed between the ground and the flight altitude. Atmospheric losses were compensated in the estimation of sound intensity levels at the aircraft. This was done using the formula given on the web page specified in reference [5].

Reference [1] described, how array shading (area-weighting) needs to be taken into account in connection with Deconvolution. Shading is applied in order to minimize the combined use of microphone signals, between which coherence has been largely lost due to air turbulence. Our array design is inspired by the one used in reference [3], and we use the same type of frequency dependent shading function, but reference [3] did not use Deconvolution. It was shown in reference [1] that for the calculation of the Point Spread Function at a given frequency  $f$  in the moving system, one must use the shading function at the Doppler shifted frequency

$Df \cdot f$  measured at the array. Here,  $Df$  is the Doppler frequency shift factor for the signal at a given microphone from a given focus point. This is because the considered frequency component  $f$  was measured at the frequency  $Df \cdot f$ , and thus shading was applied at that frequency before Delay And Sum beamforming. The applied frequency dependent shading function provides effectively equal weight per unit area over a central sub-array with radius 12 wavelengths. At that radius a smooth radial cut-off is performed by the shading function. As a result, resolution will be almost constant over a wide frequency range.

As mentioned above, our array design was inspired by the design used in reference [3], but simplified to consist of only identical radial line-arrays in order to meet the requirement for easy and fast deployment on a concrete runway. The results presented in reference [1] suggested that good results could be achieved with the simplified array design.

## 2.2 Results

All results presented in reference [1] were sound pressure contributions at the array from areas on the aircraft. In the present paper we shall be looking at estimates of the sound power radiated into the hemisphere of the array from different areas on the aircraft, assuming omnidirectional noise radiation into that hemisphere. For this estimation, correction for atmospheric losses is important except for the very low frequencies. As an example, at 5k Hz and with the relevant measurement conditions of 50% humidity and a temperature of 5°C there will be an 8.7 dB attenuation over 100 metre, [5].

Only results from a single fly-over shall be presented here and compared with results from a comparable measurement on the ground. The conditions of that flight were: Altitude = 68 m, Speed = 91 m/s, 90% engine load, high lift devices up and landing gear up. Under these conditions the engine is by far the most dominating noise contributor. During the ground based measurements, the array was pointed towards the engine nozzle, in a direction perpendicular to the longitudinal axis of the engine. To have fly-over array data that can be compared with the ground-based measurements, averaging will cover a flight track interval of length 15 m vertically above the centre of the array, but as can be seen from the picture of the aircraft in Fig. 3, the downward noise radiation from the engine intake will be more affected by the wing than the sideward radiation measured on the ground. This will influence comparison for the intake.



Fig. 3. Picture of the MU300 business jet.

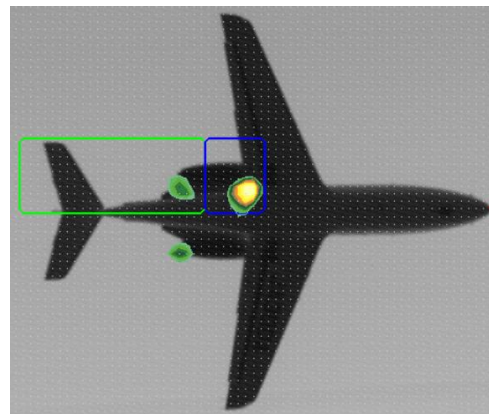


Fig. 4. Sound Intensity 315-5000 Hz

Two sound power areas were defined covering the right engine as shown in Fig. 4: one area covering the nozzle and the plume (green) and a second area covering the intake (blue), which is largely hidden above the wing. The contours represent the linearly weighted overall sound

intensity across the 1/3-octave bands from 250 to 5k Hz with a display range equal to 10 decibel. Clearly, the intake of the right engine is a dominating contributor to the noise radiation towards the array, even though the wing reflects much of the high-frequency intake noise upwards. Figure 5 shows plots of the same type as Fig. 4, but representing the single 1/3-octave bands 315, 630, 1.25k, 2.5k and 5k Hz. Display range is also 10 decibel from the peak in each individual plot. At 315 and 630 Hz the nozzle and the plume have comparable contributions, while the intake is not visible. The plume contribution being split up in two regions at 630 Hz may be an artefact of the deconvolution algorithm. At 1.25k Hz the plume contribution is vanishing, but still visible, while at 2.5k and 5k Hz it is below display range. At 2.5k Hz the intake of the right engine has a huge contribution, which is evident also from the ground based measurements in the following section. Comparison with the ground based measurements also indicates that at 5k Hz the wing is significantly reducing the downwards radiation from the intake, causing the nozzle to be the main source during fly-over. Notice the previously mentioned almost constant resolution across the considered frequency range.

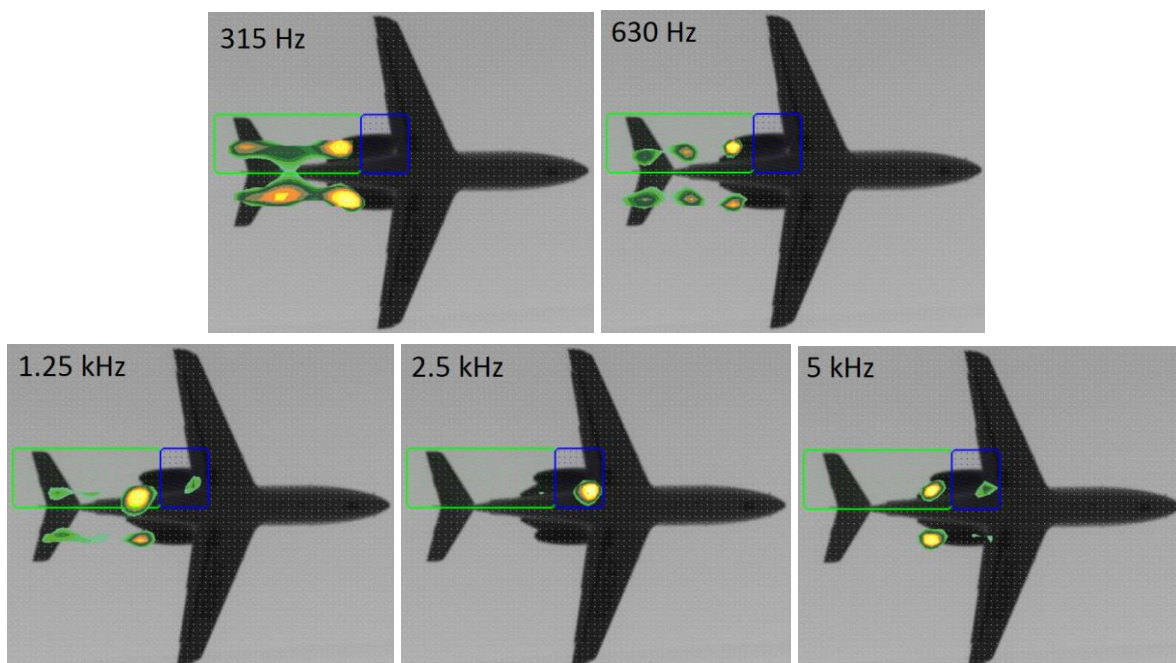


Fig. 5. Sound intensity maps for a set of 1/3-octave bands. Display range is 10 Decibel. Flight conditions: 90% engine load, high lift devices up and landing gear up.

### 3 GROUND BASED MEASUREMENTS

#### 3.1 Method and system overview

For comparison with the sub-area sound power estimates from fly-over measurements, a set of measurements were performed in 2010 with the aircraft parked on the ground and with the right engine operated at load conditions comparable to those during fly-over. Results from these measurements were published in reference [6]. Figure 6 shows the microphone pattern of the applied 60-element half wheel array, the y-axis representing distance in metre over an assumed perfectly reflecting ground plane. With the array plane perfectly vertical, imaging can be performed in the ground plane to synthesize a virtual full wheel array with 120 elements. The

array geometry has been optimized for minimum far-field sidelobe level of the virtual array up to around 6k Hz. In the context of the present paper the array has been used at a measurement distance equal to 8.8 metre.

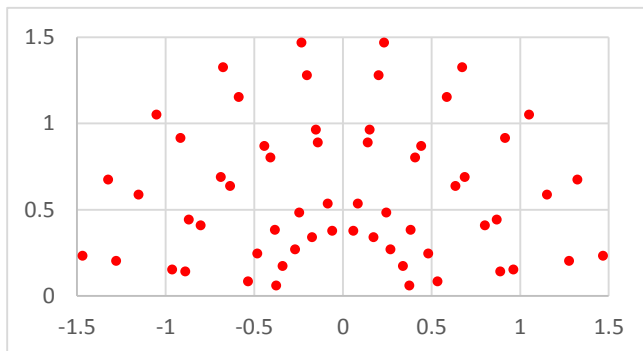


Fig. 6. Array geometry.



Fig. 7. Picture from camera in array center.

The array processing used with the half wheel array is standard Delay And Sum, followed by NNLS deconvolution. In the deconvolution process the ground reflection has to be given special attention: When computing the Point Spread Function (PSF), the point source will have an associated coherent in-phase image source in the ground plane, meaning that the PSF will be strongly dependent on the point source distance above ground. Different PSF's are therefore used for different vertical source positions, but they are assumed shift invariant in the horizontal direction. FFT-based convolution is therefore used in that direction.

Figure 7 contains a picture taken by a camera in the centre of the array. The beamforming software automatically overlays contour maps on pictures taken by that camera. Clearly, the array is pointed towards the right engine nozzle, and the array axis is perpendicular to the longitudinal axis of the right engine.

### 3.2 Results



Fig. 8. Mapping area on the aircraft with definition of two areas for sound power integration.

Figure 8 shows the mapping area on the aircraft with definition of two areas for sound power integration. The estimated sound power for these two areas will be compared with the sound power estimates for the corresponding areas in Fig. 4 and 5 for the fly-over measurement. The contour plot in Fig. 8 represents the overall sound intensity (250 Hz to 5k Hz 1/3-octave bands with linear weighting) with 10 dB display range for the case of 90% engine load like the above fly-over event. The intake is seen to be the dominating source.

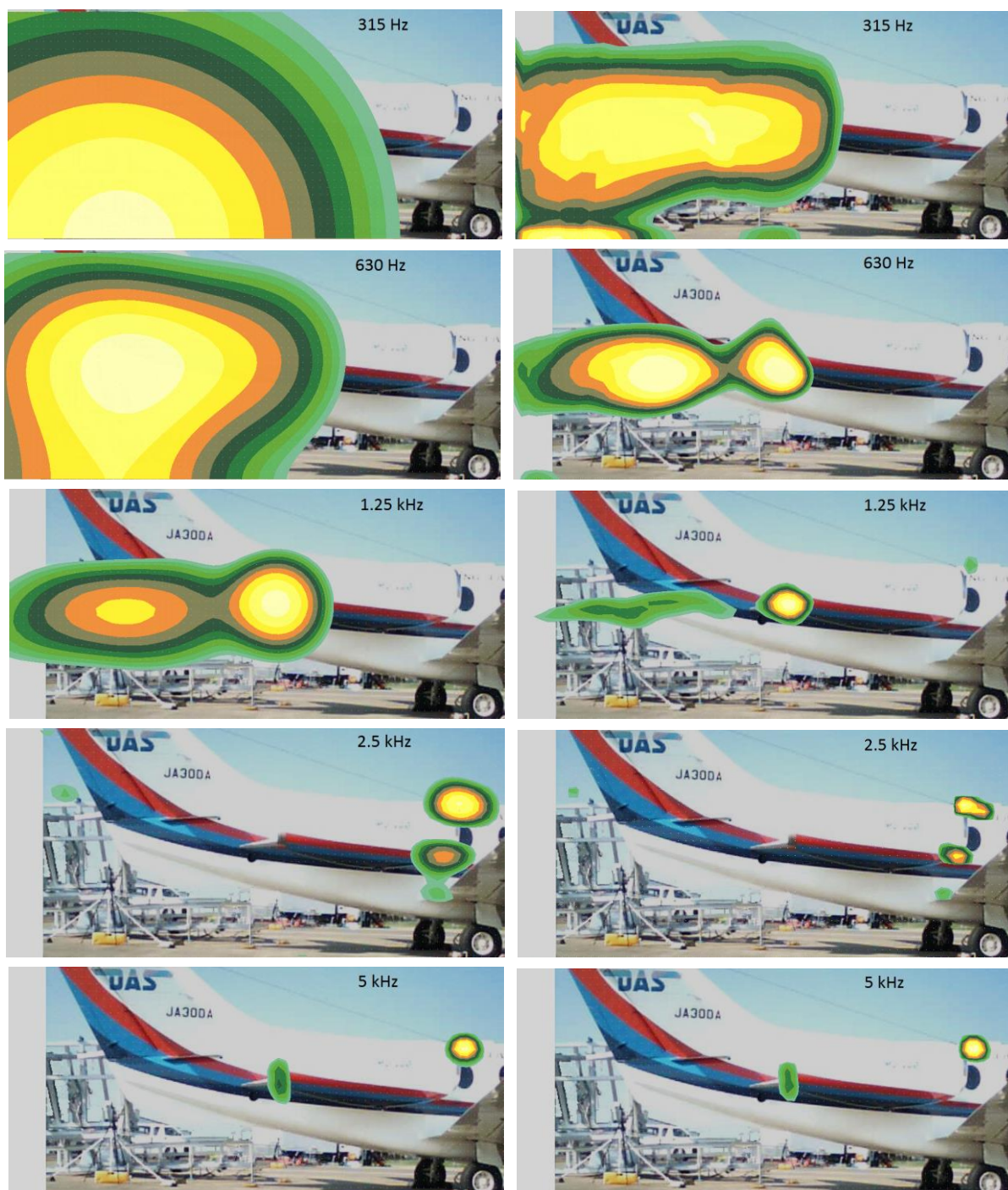


Fig. 9. Sound intensity maps with 10 dB display range. Left column: Delay And Sum output. Right column: NNLS output. Rows represent 1/3-octave bands: from the top 315, 630, 1.25k, 2.5k and 5k Hz.

Figure 9 contains sound intensity maps for the same 1/3-octave bands as Fig. 5 and for 90% engine load. The left column shows the output from Delay And Sum beamforming, while the right column presents the result after NNLS deconvolution. The rows represent different 1/3-octave bands. At 315 Hz, Delay And Sum cannot visibly resolve the real source and the image source, but NNLS manages to do that to a good extent. At 5k Hz the dominating contribution

at the array comes from the top edge of the engine intake, while the nozzle has a secondary much lower contribution than the intake. The contribution being concentrated at the top might partly explain the observation in Fig. 5 that the downwards radiation from the intake is actually weaker than the nozzle contribution during fly-over. In general, the directivity of the radiation in combination with the presence of the wing probably explain the opposite ranking in the two measurements.

#### 4 COMPARISON OF RESULTS

Figure 10 displays the sound power spectra integrated over the areas defined in Fig. 4 and 8. For the areas covering the nozzle and the plume there is good agreement up to 2k Hz between the fly-over estimates and the ground-based estimates. Above that frequency the fly-over estimates are 3 to 5 decibel lower than those measured on the ground. There can be several reasons for that. First of all the flow conditions around the engine and the plume are very different in the two cases, causing differences in the noise radiation from the shear layer. Second, the considered directions from the engine are different and, third, for the ground based measurement the reflection in the side of the fuselage may contribute positively to the measured levels, in particular at the higher frequencies.

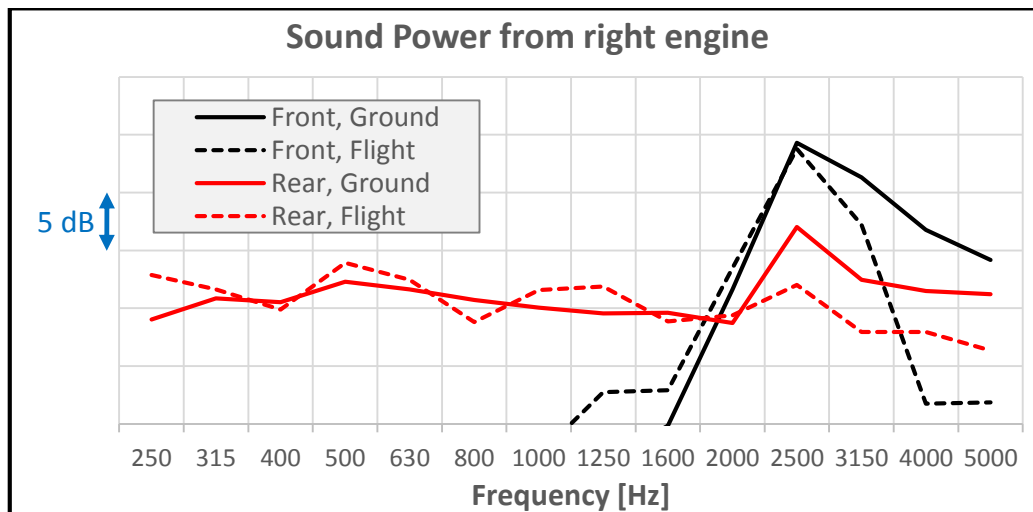


Fig. 10. Sound power 1/3-octave spectra from the ground-based (Ground) and fly-over (Flight) measurements with 90 % engine load, and for the two areas defined in Fig. 4 and 8: **Front:** Intake. **Rear:** Nozzle and plume.

For the Front area (the intake) there is good agreement up to the peak at 2.5k Hz. At that frequency, the ground-based result in Fig. 8 shows strong radiation from both the top edge and the bottom edge of the intake, and the small peak at the rear edge of the wing probably represents diffraction from a strong downwards radiation. At higher frequencies than 2.5k Hz the fly-over estimates quickly become much lower than the ground based ones. The possible reasons, which were discussed above in connection with Fig. 9, are the directivity of the noise radiation from the intake in combination with the presence of the wing.

## 5 SUMMARY

The paper has described an extension of the fly-over beamforming system presented in reference [1]. Addition of 27 peripheral microphones to the array increased the array diameter from 12 metre to 29 metre and reduced the lower limiting frequency from 700 Hz to around 300 Hz. Both arrays were designed with easy and quick deployment on a concrete runway as main design objectives, but the results show that for the extended array good performance has been achieved anyway over the frequency range from 300 Hz to 5k Hz. The presentation in reference [1] focused on estimating the contributions from different areas on the aircraft to the sound pressure at the array. Such estimates for the full aircraft could be checked directly against the measured sound pressure at the array. The present paper has focused on estimating the source strengths on the aircraft in terms of the sound power from selected areas. To support a validation of such estimates, an additional set of array measurements were performed on the ground on the same aircraft with the right engine operated at load conditions comparable with those during flight. The comparison is very good, where it should be expected to be good. Because the engine intake is largely over the wing, the downwards radiation from the intake during fly-over will differ significantly from the sideward radiation measured with the aircraft on the ground.

## ACKNOWLEDGEMENTS

The authors would like to thank Diamond Air Service Incorporation for their support in conducting the fly-over tests.

## REFERENCES

- [1] Hald, J., Ishii, Y., Ishii, T., Oinuma, H., Nagai, K., Yokoyama, Y. and Yamamoto, K., "High-resolution fly-over Beamforming using a small practical array", AIAA Paper 2012-2229.
- [2] Guérin, S. and Siller, H., "A Hybrid Time-Frequency Approach for the Noise Localization Analysis of Aircraft Fly-overs," 14th AIAA/CEAS Aeroacoustics Conference, Vancouver (Canada), 5-7 May 2008, AIAA Paper 2008-2955.
- [3] Sijtsma, P. and Stoker, R., "Determination of absolute contributions of aircraft noise components using fly-over array measurements," 10th AIAA/CEAS Aeroacoustics Conference, Manchester (UK), 10-12 May 2004, AIAA Paper 2004-2958.
- [4] Ehrenfried, K. and Koop, L., "A comparison of iterative deconvolution algorithms for the mapping of acoustic sources," 12th AIAA/CEAS Aeroacoustics Conference, Cambridge, Massachusetts (USA), 8-10 May 2006, AIAA Paper 2006-2711.
- [5] <http://www.sengpielaudio.com/AirdampingFormula.htm>.
- [6] Ishii, T., Tanaka, N., Oishi, T., Oinuma, H., Nagai, K., Nakamura, S., Tagashira, T., Ishii, Y. and Tanabe, K., "Acoustic measurement of a turbofan engine installed on a jet plane", INTERNOISE-2011, Paper No. ., 2011.